YMTHE, Volume *28*

Supplemental Information

Urinary Extracellular Vesicles Carrying Klotho Improve the Recovery of Renal Function in an Acute Tubular Injury Model

Cristina Grange, Elli Papadimitriou, Veronica Dimuccio, Cecilia Pastorino, Jordi Molina, Ryan O'Kelly, Laura J. Niedernhofer, Paul D. Robbins, Giovanni Camussi, and Benedetta Bussolati

Supplemental Methods

EV labelling

For biodistribution experiments uEVs were labelled during ultracentrifugation with liphofilic dye DiD fluorescent dye (TermoFisher Waltham. MA) as previously described.[1] One μM Vybrant Cell Tracers DiD was added during the ultracentrifugation procedure. Then, labelled uEVs were washed twice by ultracentrifugation in PBS (Lonza). Similar procedure was followed in the absence of uEV in order to collect potential dye aggregates to set the fluorescent background.

uEVs floating purification

To increase the purity of uEVs and separate vesicles from aggregates a floating protocol through a sucrose gradient was applied.[2] Briefly, ultracentrifuged EVs were resuspended in 1.35 ml of buffer (0.25 M sucrose, 10 mM Tris pH 8 and 1 mM EDTA, all products purchased by Sigma-Aldrich, St. Louis, MI), transferred to a SW55Ti rotor tube (Beckman Coulter) and mixed with 60% stock solution of Optiprep (Sigma-Aldrich) in a 1:1 ratio. Next, 1.2 ml of 20% Optiprep solution was layered on top, followed by 1.1 ml of 10% Optiprep solution. The tubes were then ultracentrifuged at 350.000 g for 1 hour at +4°C with “no brake” deceleration. The next day five fractions of 1 ml each were collected from the top of the tubes, each fraction was diluted in 25 ml PBS (Lonza) and ultracentrifuged at 100.000 g (rotor type 70Ti) for two hours at +4°C to pellet the EVs. The highest fraction, containing pure EVs, as assessed by NanoSight analysis, was then resuspended in 200 μl of DMEM (Lonza) plus 1% DMSO (Sigma-Aldrich) to allow freezing storage in -80°C until use.

EV quantification

EVs were analysed by nanoparticle tracking analysis (NTA) using the NanoSight NS300 system (NanoSight Ltd Salisbury, UK) configured with a Blue 488 nm laser and a high sensitivity digital camera system OrcaFlash 2.8. Hamamatsu C1 1440 (NanoSight Ltd). Briefly, EVs stored in -80°C were thawed, strongly vortexed and properly diluted in physiologic solution (Fresenius Kabi, Bad Homburg, Germany) previously filtered with 0.1 μm filter (Merck Millipore). For each sample, three videos of 30-second duration were recorded. The settings of acquisition and analysis were

optimized and kept constant between samples. The final analysis reported mean size and particles concentration.

Electron Microscopy

uEVs were loaded onto 200 mesh nickel formvar carbon coated grids (Electron Microscopy Science) for 20 min for transmission electron microscopy, followed by fixation in a 2.5% glutaraldehyde/2% sucrose solution. Samples were washed in distilled water, negatively stained with NanoVan (Nanoprobes, Yaphank) and examined by a Jeol JEM 1010 electron microscope (Joel, USA).

Cytofluorimetric analysis

As EVs are too small for FACScan analysis, analysis was performed on EVs bound to surfactant-free white aldehyde/sulfate latex beads 4% w/v 4 μm diameter (Molecular Probes, Invitrogen Carlsbad, CA). Five μl of beads were incubated with 30 μg of EVs for 30 min at room temperature and then for 30 min at +4°C.[3] Adsorbed EVs were divided in different vials and incubated with antibodies for 15 min at +4°C. The adsorbed EVs were then washed and analyzed with a FACSCalibur and CellQuest software (Becton Dickinson Bioscience Pharmingen. Franklyn Lake, NJ). Flow cytometry was performed using anti-human fluorescent-conjugated monoclonal antibodies (1:50 dilution): Podocalyxin-APC (PDX) (R&D, Minneapolis, #FAB1658A). CD24-FITC (Miltenyi, Bergisch Gladbach, Germany, #130-095-952). CD63-APC (Miltenyi, #130-100-173). VEGFR2-APC (VR2) (Miltenyi, #130-093-601). CD81-PE (Becton Dickinson, Franklin Lakes, New Jersey, #555676). CD45-FITC (Becton Dickinson, #555482) and CD42b-FITC (Becton Dickinson, #555472). Aquaporin-1 (AQP1) (Santa Cruz Biotechnology, Dallas, TX, #sc-20810) and Aquaporin-2 (AQP2) (Santa Cruz, #sc-28629) were conjugated to an Alexa Fluor® 488 dye through the Alexa Fuor® Antibody Labeling Kit (Molecular Probes. #A20181) following the manufacturer's instructions and used at 1:250 dilution. Gating was performed on the physical parameters dot plot. Controls were represented by EVs adsorbed on beads and marked with FITC-, PE- or APC- conjugated Mouse IgG1 Isotypes (all purchased by Miltenyi, #130-092-213, #130-

092-212 and #130-092-214). Beads with antibodies in the absence of EVs did not show positive fluorescence (not shown).

uEV miRNA content

Total RNA was extracted from a pool of uEVs deriving from 8 litres of urine. uEVs were lysed in Trizol (Ambion, Waltham, MA) and RNA extracted using miRNeasy kit (Qiagen Hilden, Germany) following the manufacturer's protocol. After isolation, total RNA concentration was evaluated using a ND-1000 spectrophotometer (Nanodrop ND-1000, Waltham, MA). Sixty nanograms of RNA were precipitated and pre-amplified prior to miRNA quantification. 380 different miRNAs expression was evaluated by quantitative real-time PCR (qRT-PCR) using Taqman Array MicroRNA card B (v3.0) according to Megaplex protocol. Quantification was performed using a QuantStudio 12K Flex Real-Time PCR System (Applied Biosystems, Foster City, CA). Cycle threshold (Ct) values were analysed by QuantStudio 12K Flex software (Applied Biosystems) using global normalization. MiRNAs with raw Ct values higher than 35 were not included in the analysis.

For qRT-PCR, RNA was purified from uEV using the *mirVana* miRNA Isolation Kit (Ambion) according to the manufacturer's protocol. First-strand cDNA was produced from 200 ng of total RNA using the miScript Reverse Trascription kit (Qiagen). MiRNA expression analysis was performed by qRT-PCR in 20 µl reaction mixture containing 4 ng of cDNA template, the sequence-specific oligonucleotide primers (purchased from MWG-Biotech, Ebersberg, Germany) and the miScript SYBR Green PCR kit (Qiagen). The snoRNA RNU6B was used as normalizer. Relative quantification of the products was performed using a 96-well StepOne Real-Time System (Applied Biosystems). miRNAs with raw *C*t values greater than 35 were not included in the analysis. Sequence specific oligonucleotide primers are reported below.

	Sequences
RNU6B	5′-CGCAAGGATGACACGCAA -3′
Mir-30a-3p	5′-CTTTCAGTCGGATGTTTGCAGC-3′
Mir-30e-3p	5′-CTTTCAGTCGGATGTTTACAGC-3′

Mir-30a-5p	5′-TGTAAACATCCTCGACTGGAA-3′
Mir-30d-3p	5′-CTTTCAGTCAGATGTTTGCTGC-3′
Mir-10b-3p	5′-ACAGATTCGATTCTAGGGGAAT-3′
Mir-664a-3p	5′-TATTCATTTATCCCCAGCCTACA-3′
Mir-151a-3p	5′-CTAGACTGAAGCTCCTTGAGG-3′
Mir-1260a	5′-ATCCCACCTCTGCCACCA-3′
Mir-31-3p	5′-TGCTATGCCAACATATTGCCAT-3′
Mir-151a-5p	5′-TCGAGGAGCTCACAGTCTAGT-3′

Funrich analysis tool was used to perform target prediction analysis.[4] Network analysis to define the associated pathways of the predictive genes was generated by the FunRich interaction plug-in (p-value <0.01 in the enriched pathways). A filter of a minimum of six interactions among different nodes was applied.

Blood analysis for renal function

Blood samples for the quantification of serum creatinine and BUN were performed using a colorimetric microplate assays (Quantichrom Creatinine Assay, BioAssay Systems and Quantichrom Urea Assay, BioAssay Systems, Hayward, CA) following the manufacturer's guidelines. Creatinine kinase activity was also quantified using the Cobas e 411 analyser (Roche, Basel, Switzerland), as previously described.[5]

Morphological Studies

For renal histology, 5 μm thick paraffin kidney sections were routinely stained with haematoxylin and eosin (Merck Millipore). Luminal hyaline casts and tubular necrosis (denudation of tubular basement membrane) were assessed in non-overlapping fields (up to 10 for each section) using a 20× objective (high power field, HPF).[4] Number of casts and tubular profiles showing necrosis was recorded in a single blind fashion. The presence of ferric iron within renal tissue was evaluated using "PEARLS for ferric iron" staining (Bi-Optica, Milano, IT) following the manufacture's protocol.

Immunohistochemistry for the detection of proliferation of tubular cells was performed. Kidney sections of paraffin-embedded samples were stained with a monoclonal anti-PCNA antibody (Proliferating Cell Nuclear Antigen) (Santa Cruz). Apoptosis was evaluated using the TUNEL assay analysis (ApopTagOncor, Gaithersburg, MD), following the manufacture's protocol. Number of PCNA-positive cells and of TUNEL-positive nuclei was evaluated by counting the number of positive nuclei per field in 10 randomly chosen sections of kidney cortex (20× magnification) using ImageJ software. Immunohistochemistry for the detection of Klotho was performed using a polyclonal anti-Klotho antibody (Abcam, Cambridge, UK). Immunoperoxidase reactions were performed using anti-rabbit HRP antibody (Pierce, Rockford, IL).

Optical imaging and biodistribution of uEVs

Nude mice were used to evaluate the accumulation of labelled uEVs within injured kidneys. Healthy and AKI mice were intravenously injected with $1.5x10^{10}$ DiD-labeled uEVs (n=6). Three healthy mice and 3 AKI mice received DID dye (Molecular Probes, Invitrogen) alone in order to set fluorescence background measurement. All studies were performed with IVIS 200 small animal imaging system (PerkinElmer. Waltham. MA) using excitation filter at 640 nm and emission filter at 700 nm. Fluorescence emission was normalized to photons per second per centimetre squared per steradian (p/sec/cm^2/sr). Mice were anesthetized with 2.5% isoflurane (Merial, Lyon, France) and images were acquired in the prone position after four hours post EV injection. Then, mice were sacrificed and dissected kidneys were imaged immediately as previously described.[1] The fluorescence signal was quantified in the kidney region in ROI draw freehand. The relative mean fluorescence intensity of each ROI was obtained by subtracting the mean fluorescence intensity of the corresponding ROI of the fluorescence intensity of mice treated with DiD alone. Data were expressed as the average radiance ±SD. Images were acquired and analysed using Living Image 4.0 software (Perkin Elmer).

Tissue RNA isolation – Real Time PCR

For the isolation of RNA from mouse kidneys, pieces of around 50 mg of renal tissue were homogenized in 1 ml of Trizol Reagent (Ambion) according to the manufacturer's protocol. RNA was then quantified spectrophotometrically by Nanodrop. First-strand cDNA was produced from 200 ng of total RNA using the High Capacity cDNA Reverse Transcription Kit (Applied Biosystems). For gene expression analysis, qRT-PCR was performed in 20 μl reaction mixture containing 5 ng of cDNA template, the sequence-specific oligonucleotide primers (purchased from MWG-Biotech) and the Power SYBR Green PCR Master Mix (Applied Biosystems). mGAPDH was used as housekeeping normalizer. Fold change expression respect to 1 for Vehicle was calculated for all samples. The sequence-specific oligonucleotide primers used are shown in the following table.

	Forward	Reverse
mGAPDH	5′-AACTTTGGCATTGTGGAAGG-3′	5′-ACACATTGGGGGTAGGAACA-3′
mNGAL	5′-TGCACAGGTATCCTCAGGTACAGA-3′	5′-GGAAAAATACCATGGCGAACTG-3′
mPAI	5′-AGTCAATGAGAAGGGCACAGCT-3′	5′-TAGGTCCCGCTGGACAAAGAT-3′
mSOX9	5′-AGTACCCGCATCTGCACAAC-3′	5′-ACGAAGGGTCTCTTCTCGCT-3′
mCASP3	5′-CCATAAGAGCACTGGAATGTCATC-3′	5′-TCCAAAATGTCTTCACGAGTAAGATC-3′
mASMA	5′-GAGGCACCACTGAACCCTAA-3′	5′-CATCTCCAGAGTCCAGCACA-3′
mSMAD1	5′-TTCAGATGCCAGCTGACACAC-3′	5′-CCTCTGCTGATTTCAGCGG -3′
mSMAD2	5′-TGAGACCCCAGTCTTGCCTC-3′	5′-CTGTGGCTCAATTCCTGCTG-3′
mc-Myc	5′-ACCAGCAGCGACTCTGAAGAAG-3′	5′-ATGGAGATGAGCCCGACTCC-3′
mCCND1	5′-CCTGGATGCTGGAGGTCTGT-3′	5′-CCAGGGACAGGAAGCGGT-3′
mCTGF	5′-CTTCTGCGATTTCGGCTCC-3′	5′-TGCTTTGGAAGGACTCACCG-3′
mTNF-a	5′-CATCTTCTCAAAATTCGAGTGACAA-3′	5′-TGGGAGTAGACAAGGTACAACCC-3′
mNF-kB	5′-ACAGGTCAAAATTTGCAACTATGTG-3′	5′-TGCATACCCCGTCCTCACA-3′
mIL1-beta	5′-CAACCAACAAGTGATATTCTCCATG-3′	5′-GATCCACACTCTCCAGCTGCA-3′
mIL6	5′-ACCAGAGGAAATTTTCAATAGGC-3′	5′-TGATGCACTTGCAGAAAACA-3′
h-KLOTHO	5′-GGAAACCTTAAAAGCCATCAAGCT-3′	5′-GAAGACTTTGGCAACAACATC TTG T-3′

miRNA transfer in renal tissue

miRNA transfer in renal tissue was evaluated by qRT-PCR using the miScript SYBR Green PCR kit (Qiagen). The snoRNA RNU6B was used as normalizer. Relative quantification of the products

was performed using a 96-well StepOne Real-Time System (Applied Biosystems). Fold change expression in respect to Vehicle was calculated for all samples. The sequence-specific oligonucleotide primers used are shown in table in “uEV miRNA content” section.

Western Blot

For protein analysis of renal tissue, pieces of around 50 mg were homogenized in 1 ml of RIPA buffer, containing 1% of Phosphatase Inhibitor Cocktails. Protease Inhibitors and PMSF (all products purchased by Sigma-Aldrich). Proteins from EVs were extracted using the same lysis buffer, while protein concentration was estimated by Bradford (Bio-Rad, Hercules, CA) quantification. Ten μg of EV-lysates and 50 μg of renal tissue lysates were loaded on Mini-PROTEAN TGX pre-cast electrophoresis gels (Bio-Rad). Proteins were subsequently transferred on iBlot nitrocellulose membranes (Invitrogen) and blotted with antibodies against Klotho (Abcam. #181373), Vinculin (Sigma-Aldrich, #V4505), AQP1 (Santa Cruz Biotechnology, sc-20810), AQP2 (Santa Cruz Biotechnology, sc-28629), CD63 (Santa Cruz Biotechnology, sc-15363) and Calreticulin (Cell Signaling, Danvers, Massachusetts, #2891). Chemiluminescent signal was detected using the ECL substrate (Bio-Rad).

Supplemental References:

1. Grange C. Tapparo M. Bruno S. Chatterjee D. Quesenberry PJ. Tetta C. et al.: Biodistribution of mesenchymal stem cell-derived extracellular vesicles in a model of acute kidney injury monitored by optical imaging. Int J Mol Med 33: 1055-1063. 2014.
2. Kowal J. Arras G. Colombo M. Jouve M. Morath JP. Primdal-Bengtson B. et al.: Proteomic comparison defines novel markers to characterize heterogeneous populations of extracellular vesicle subtypes. Proc Natl Acad Sci USA 113: E968–977. 2016.
3. Dimuccio V. Ranghino A. Praticò Barbato L. Fop F. Biancone L. Camussi G. et al.: Urinary CD133+ extracellular vesicles are decreased in kidney transplanted patients with slow graft function and vascular damage. PLoS One 9(8): e104490. 2014.
4. Bruno S. Tapparo M. Collino F. Chiabotto G. Deregibus MC. Soares Lindoso R. et al.: Renal Regenerative Potential of Different Extracellular Vesicle Populations Derived from Bone Marrow Mesenchymal Stromal Cells. Tissue Eng Part A 23: 1262-1273. 2017.
5. Moggio A. Geraci S. Boido A. Sticht C. Gretz N. Bussolati B: Assessment of an acute kidney injury in rhabdomyolytic mice by transcutaneous measurement of sinistrin excretion. Nephrol Dial Transplant 1;32(7):1167-1175. 2017.

Supplemental Figures

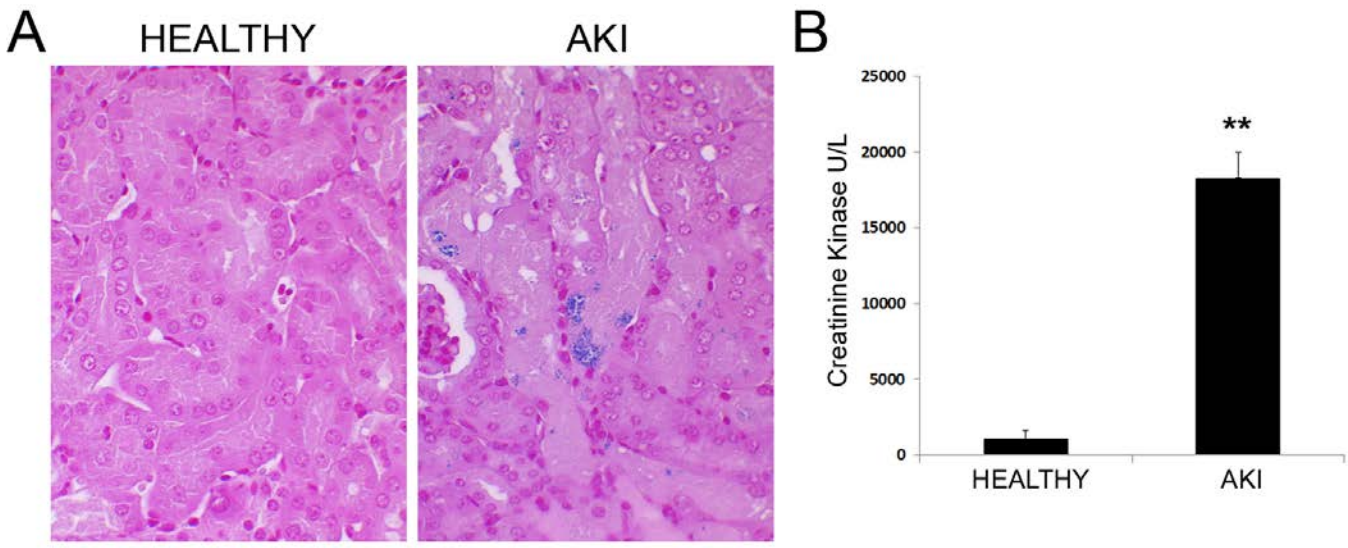

Supplemental Figure 1. Assessment of glycerol induced rhabdomyolysis. (A) Representative images of Pearls staining showing iron deposits (in blue) on renal tissue of Healthy and AKI mice. Original magnification: x200. (B) Histograms representing the level of the muscle damage marker creatinine kinase (U/L) in Healthy and AKI mice, 24 hours post glycerol injection (n=3).

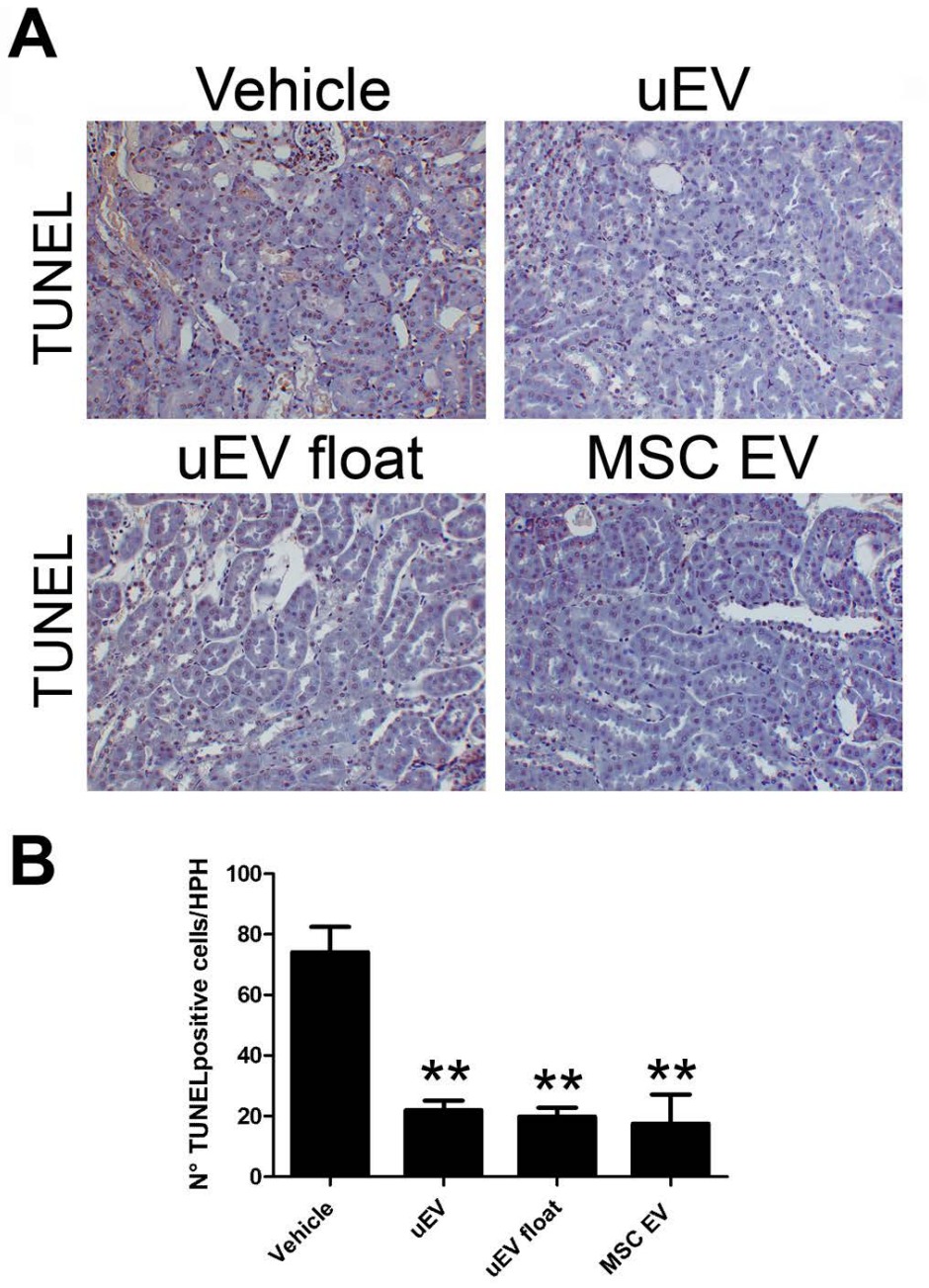

Supplemental Figure 2. uEVs abrogate tubular cell apoptosis. (A) Representative micrographs showing TUNEL positive cells in kidney tissues from AKI mice injected with saline (Vehicle), uEVs, uEVs float and MSC EVs, at day 3 after damage. Original magnification: x200. (B) Quantification of TUNEL positive cells in AKI mice treated or not (Vehicle) with EVs at day 3 post damage. Data are expressed as the mean ±SEM of the count of 10 fields/section (n=4 mice for each group). ANOVA with Dunnet's multicomparison test was performed: **p<0.001 versus Vehicle.

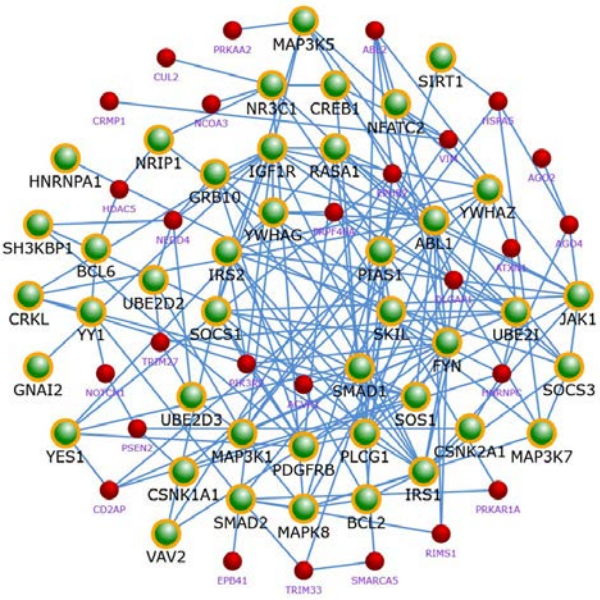

Supplemental Figure 3. Network interactome analysis. Network interactome analysis of the uEVs predictive genes targeted by the four transferred miRNAs. The yellow node boundary represents the selected candidate molecules associated with the following highly over-represented pro regenerative pathways: proteoglycan–syndecan signalling events, IGF-1 and HGF ($p<0.001$).

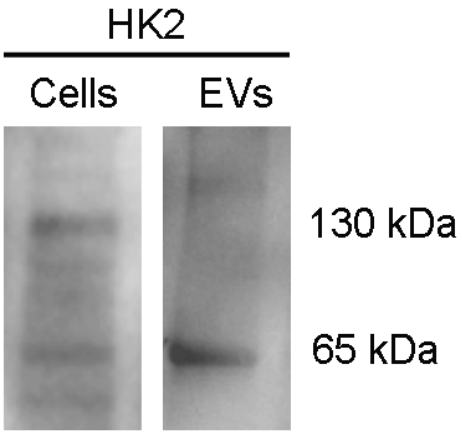

Supplemental Figure 4. Klotho expression in HK2 cells and derived EVs. Representative Western blot showing the presence of Klotho in HK2 cells and isolated EVs.

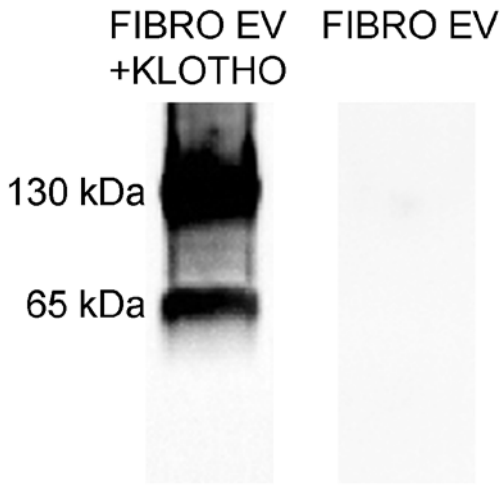

Supplemental Figure 5. Engineering of fibroblast derived EVs with human recombinant Klotho. Representative western blot showing the efficient engineering of FIBRO EVs with human recombinant Klotho, absent in native FIBRO EVs.

Supplemental Table 1. miRNAs expressed by uEVs by Array. MicroRNAs expressed by uEVs listed in the order of expression level.

miRNAs expressed by uEVs			
miRNAs	Average CT value	miRNAs	Average CT value
hsa-miR-30a-3p	16.121	hsa-miR-935	30.147
hsa-miR-30e-3p	16.845	hsa-miR-1247-5p	30.366
hsa-miR-30a-5p	17.253	hsa-miR-20b-3p	30.374
hsa-miR-30d-3p	19.445	hsa-miR-148a-5p	30.393
hsa-miR-10b-3p	19.578	hsa-miR-136-3p	30.412
hsa-miR-664a-3p	19.732	hsa-miR-1251-5p	30.419
hsa-miR-151a-3p	20.843	hsa-miR-92a-1-5p	30.468
hsa-miR-1260a	21.445	hsa-miR-944	30.468
hsa-miR-31-3p	22.564	hsa-miR-765	30.483
hsa-miR-151a-5p	22.980	hsa-miR-190b	30.519
hsa-miR-7-1-3p	23.192	hsa-miR-483-3p	30.738
hsa-miR-29c-5p	23.716	hsa-miR-141-5p	30.889
hsa-miR-200a-5p	23.800	hsa-miR-129-1-3p	30.952
hsa-miR-766-3p	23.857	hsa-miR-18a-3p	31.169
hsa-miR-625-3p	23.866	hsa-miR-1303	31.231
hsa-miR-93-3p	24.284	hsa-miR-892b	31.314
hsa-miR-378a-3p	24.363	hsa-miR-378a-5p	31.321
hsa-miR-1180-3p	24.505	hsa-miR-638	31.361
hsa-miR-181a-2-3p	24.667	hsa-miR-24-2-5p	31.365
hsa-miR-99b-3p	24.747	hsa-let-7c-3p	31.371
hsa-miR-425-3p	24.753	hsa-miR-1236-3p	31.387
hsa-miR-183-3p	24.832	hsa-miR-939-5p	31.397
hsa-miR-222-5p	24.846	hsa-miR-1296-5p	31.401
hsa-miR-577	24.853	hsa-miR-616-5p	31.466
hsa-miR-34a-3p	24.985	hsa-miR-1208	31.559
hsa-miR-1226-5p	2.5068	hsa-miR-33a-3p	31.612
hsa-miR-628-3p	25.087	hsa-miR-15a-3p	31.642
hsa-miR-26a-1-3p	25.093	hsa-miR-550a-3p	31.659
hsa-miR-590-3p	25.159	hsa-miR-196a-3p	31.736
hsa-miR-26b-3p	25.165	hsa-miR-1249-3p	31.891
hsa-miR-1271-5p	25.172	hsa-let-7a-3p	31.928
hsa-miR-335-3p	25.251	hsa-let-7f-2-3p	31.954
hsa-miR-409-3p	25.292	hsa-miR-144-3p	31.997
hsa-miR-629-3p	25.364	hsa-miR-125b-1-3p	32.005
hsa-miR-22-5p	25.389	hsa-miR-223-5p	32.047
hsa-miR-99a-3p	25.509	hsa-miR-520c-3p	32.065
hsa-miR-27a-5p	25.517	hsa-let-7i-3p	32.087
hsa-let-7d-3p	25.549	hsa-miR-1224-3p	32.103
hsa-miR-34b-3p	2.5629	hsa-miR-1244	32.116
hsa-miR-650	25.660	hsa-miR-24-1-5p	32.144
hsa-miR-27b-5p	25.802	hsa-let-7e-3p	32.165
hsa-miR-125b-2-3p	26.101	hsa-miR-1183	32.235
hsa-miR-9-3p	26.103	hsa-miR-144-5p	32.292
hsa-miR-20a-3p	26.144	hsa-miR-938	32.321
hsa-miR-130b-5p	26.316	hsa-miR-875-5p	32.352

hsa-miR-424-3p	26.336	hsa-let-7g-3p	32.359
hsa-miR-340-3p	26.355	hsa-miR-543	3.2391
hsa-miR-505-5p	26.465	hsa-miR-1276	32.449
hsa-miR-10a-3p	26.473	hsa-miR-200c-5p	32.474
hsa-miR-1275	26.513	hsa-miR-663b	32.547
hsa-miR-206	26.570	hsa-miR-221-5p	32.591
hsa-miR-1290	26.587	hsa-miR-769-3p	32.638
hsa-miR-769-5p	26.659	hsa-miR-639	32.683
hsa-miR-320b	26.698	hsa-miR-16-1-3p	32.775
hsa-miR-193b-5p	2.6713	hsa-miR-520d-3p	32.780
hsa-miR-1270	27.018	hsa-miR-1179	32.816
hsa-miR-589-3p	27.069	hsa-miR-374a-3p	32.825
hsa-miR-584-5p	27.179	hsa-miR-596	32.827
hsa-miR-942-5p	27.352	hsa-miR-100-3p	32.873
hsa-miR-148b-5p	27.529	hsa-miR-545-5p	32.982
hsa-miR-1233-3p	27.553	hsa-miR-1292-5p	32.992
hsa-miR-500a-3p	27.555	hsa-miR-92b-5p	33.104
hsa-miR-192-3p	27.563	hsa-miR-1301-3p	33.111
hsa-miR-454-5p	27.671	hsa-miR-550a-5p	33.178
hsa-miR-181c-3p	27.768	hsa-miR-581	33.179
hsa-miR-30d-5p	27.813	hsa-miR-572	33.187
hsa-miR-432-5p	27.889	hsa-miR-7-5p	33.283
hsa-miR-19b-1-5p	28.001	hsa-miR-770-5p	33.303
hsa-miR-29a-5p	28.013	hsa-miR-101-5p	33.351
hsa-miR-934	28.069	hsa-miR-1225-3p	33.448
hsa-miR-1269a	28.179	hsa-miR-1262	33.521
hsa-miR-191-3p	28.207	hsa-miR-661	33.591
hsa-miR-15b-3p	28.208	hsa-miR-34b-5p	33.598
hsa-miR-571	28.214	hsa-miR-548i	33.599
hsa-miR-622	28.297	hsa-miR-497-5p	33.654
hsa-miR-361-3p	28.301	hsa-miR-1305	33.756
hsa-miR-30c-2-3p	28.364	hsa-miR-1267	33.822
hsa-miR-135b-3p	28.381	hsa-miR-943	33.830
hsa-miR-194-3p	28.409	hsa-miR-302d-5p	33.913
hsa-miR-941	28.549	hsa-miR-513c-5p	33.968
hsa-miR-200b-5p	28.778	hsa-miR-1265	34.069
hsa-miR-592	28.893	hsa-miR-23b-5p	34.075
hsa-let-7f-1-3p	28.893	hsa-miR-17-3p	34.352
hsa-miR-33a-5p	28.953	hsa-miR-551b-5p	34.363
hsa-miR-1254	28.972	hsa-miR-604	34.392
hsa-miR-1227-3p	28.979	hsa-miR-643	34.461
hsa-miR-363-5p	29.141	hsa-miR-30c-1-3p	34.473
hsa-miR-138-2-3p	29.307	hsa-miR-26a-2-3p	34.708
hsa-miR-29b-2-5p	29.315	hsa-miR-668-3p	3.4709
hsa-miR-181a-3p	29.466	hsa-miR-937-3p	34.753
hsa-miR-744-3p	29.599	hsa-miR-1263	34.754
hsa-let-7b-3p	29.606	hsa-miR-624-5p	34.803
hsa-miR-126-5p	29.614	hsa-miR-516-3p	34.869
hsa-miR-1825	2.9637	hsa-miR-549a	34.978
hsa-miR-25-5p	29.786	hsa-miR-601	35.067
hsa-miR-1298-5p	29.791	hsa-miR-374b-3p	35.166
hsa-miR-1285-3p	29.895	hsa-miR-302a-5p	35.169
hsa-miR-7-2-3p	29.977	hsa-miR-1243	35.272
hsa-miR-21-3p	30.145	hsa-miR-432-3p	3.5274
		hsa-miR-767-5p	35.630

Supplemental Table 2. Mean CT values of the 10 most expressed miRNAs in uEVs evaluated by qRT-PCR. Data are mean ±SD of three different experiments using three different EV pools.

uEVs	CT	SD
hsa-miR-30a-3p	23.80	±0.14
hsa-miR-30e-3p	24.73	±0.18
hsa-miR-30a-5p	19.89	±0.04
hsa-miR-30d-3p	29.73	±0.18
hsa-miR-10b-3p	31.71	±0.19
hsa-miR-664a-3p	25.99	±0.22
hsa-miR-151a-3p	26.87	±0.05
hsa-miR-1260a	20.33	±0.37
hsa-miR-31-3p	32.61	±0.29
hsa-miR-151a-5p	24.68	±0.22
RNU6B	28.28	±0.47